IPPP/14/94
DCPT/14/188

Constraining Dark Sectors at Colliders: Beyond the Effective Theory Approach

Philip Harris,[1] Valentin V. Khoze,[2] Michael Spannowsky,[2] and Ciaran Williams[3,4]

[1] *CERN, CH-1211 Geneva 23, Switzerland*
[2] *Institute for Particle Physics Phenomenology, Department of Physics, Durham University, Durham DH1 3LE, United Kingdom*
[3] *Niels Bohr Institute, University of Copenhagen, Blegdamsvej 17, DK-2100 Copenhagen, Denmark*
[4] *Department of Physics, University at Buffalo The State University of New York, Buffalo, NY 14260-1500, USA*

philip.coleman.harris@cern.ch, valya.khoze@durham.ac.uk, michael.spannowsky@durham.ac.uk, ciaran@nbi.dk

arXiv:1411.0535v2 [hep-ph] 5 Feb 2015

We outline and investigate a set of benchmark simplified models with the aim of providing a minimal simple framework for an interpretation of the existing and forthcoming searches of dark matter particles at the LHC. The simplified models we consider provide microscopic QFT descriptions of interactions between the Standard Model partons and the dark sector particles mediated by the four basic types of messenger fields: scalar, pseudo-scalar, vector or axial-vector. Our benchmark models are characterised by four to five parameters, including the mediator mass and width, the dark matter mass and an effective coupling(s). In the gluon fusion production channel we resolve the top-quark in the loop and compute full top-mass effects for scalar and pseudo-scalar messengers. We show the LHC limits and reach at 8 and 14 TeV for models with all four messenger types. We also outline the complementarity of direct detection, indirect detection and LHC bounds for dark matter searches. Finally, we investigate the effects which arise from extending the simplified model to include potential new physics contributions in production. Using the scalar mediator as an example we study the impact of heavy new physics loops which interfere with the top mediated loops. Our computations are performed within the MCFM framework and we provide fully flexible public Monte Carlo implementation.

I. INTRODUCTION

Many extensions of the Standard Model predict the existence of dark particles that can be produced in collisions of ordinary matter, but are not directly measurable at the LHC's multipurpose experiments. When measuring the radiation in a scattering event, dark particles would manifest themselves as missing transverse energy i.e. as an imbalance of the total transverse momentum in the event. Dark particles constitute the dark sector which plays a special role in any comprehensive beyond the Standard Model (BSM) description of particle physics: some of the dark sector particles can be cosmologically stable[1] and as such they give rise to the dark matter. Non-trivial dark sectors can also contain massless vector fields which contribute to the dark radiation in the Universe. The fact that the dark matter (DM) and dark radiation give the dominant contributions to the matter and radiation in the Universe is one of the clearest indications that the Standard Model is incomplete and new physics effects must be present in a more fundamental theory of particle interactions.

While dark sectors can be complex, resulting in a rich and varied BSM phenomenology, they have one universal feature which is of particular importance: dark matter particles can interact with visible matter by exchanging a mediator field. When studying scenarios for the production of dark particles at colliders, we consider processes in which a mediator is produced initially in the course of the hadron-hadron collision. This mediator then subsequently decays, either back to SM degrees of freedom or into the dark sector particles. These latter channels will correspond to events with missing transverse energy at colliders. There is no a priori requirement that the mediator decays directly into cosmologically stable DM; all decays into dark particles which are stable at collider scales or do not result in measured displaced vertices will manifest themselves as missing energy. In this sense it is the production and the role of the mediator particle(s) which is of key importance in the collider searches for dark sectors; the actual dark matter is a derivative.

Depending on the nature of the mediator field (arguably the most interesting choices being a vector, axial-vector, scalar or a pseudo-scalar) different mediator production mechanisms can occur. For vectors and axial-vectors, a common assumption is that the dominant production mechanism is the quark-antiquark annihilation at tree-level. For scalars and pseudo-scalars on the other hand, the gluon fusion processes are more relevant. This is inspired by

[1] This is usually a result of of an automatic or imposed discrete symmetry present in the dark sector.

the recent Higgs discovery and assumes that the coupling strength of the new scalars to Standard Model fermions is proportional to their SM Yukawa couplings.

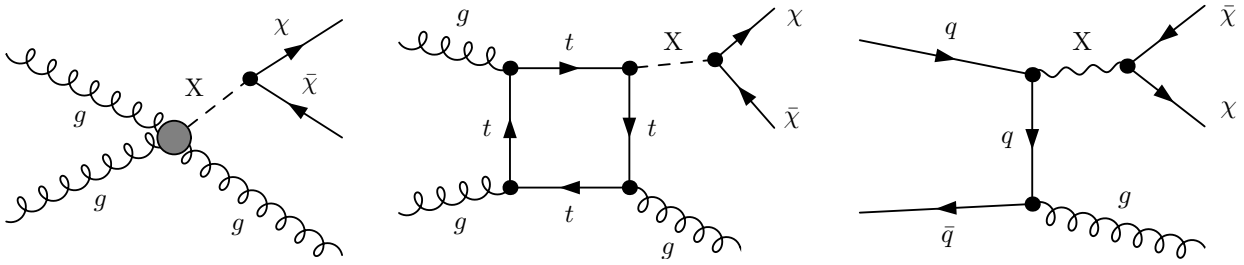

FIG. 1: Representative Feynman graphs for gluon and quark induced mono-jet processes. The particle X can be either a scalar, pseudo-scalar, vector or axial-vector mediator. The left diagram shows an effective operator approximation of the mediator coupling to gluons. The middle graph represents the full description of the same process, including the fermion mass dependence in the loop, while the right graph depicts a mediator produced in a quark-anti-quark annihilation.

Inferring the existence of dark particles in collider experiments requires them to recoil against visible radiation. Since the recoil object need not be essential in the interaction which produces the mediator, a natural candidate for the tagging object is the emission of initial state radiation, which occurs at a high rate at the LHC. In these mono-jet signatures a hard jet recoils against the invisible particles. Events with several hard jets are often vetoed, leaving Z/W+jets as major Standard Model backgrounds. In these events the transverse momentum of the jet sets the energy scale of the hard interaction.

The mediating particle can couple directly or indirectly to the initial state patrons, representative diagrams are shown in Fig. 1. The diagram on the far right of Fig. 1 represents an example in which the mediator-SM interaction proceeds via a tree-level interaction with quarks. The mediator can also couple to initial states indirectly, in these instances the underlying production mechanism corresponds to loop-induced process, the middle diagram in Fig. 1 illustrates this scenario. The propagating loop particle can be integrated out, resulting in an effective dimension-5 operator, illustrated in the left most diagram of Fig. 1. This prescription is invalid if $p_{T,j} \gtrsim \mathcal{O}(m_X)$, where m_X is the mass of the loop particle. In the case of the top quark, this can readily be achieved. On the other hand, heavy colored states which couple to the mediator can be integrated out provided $\Lambda_{\rm NP}$ is much larger than the energy scale where the operator is probed.

To be able to probe new physics models with particle masses below the characteristic interaction scale of the hard interaction, so-called simplified models were proposed [1] which only make assumptions on the quantum numbers of particles involved in the minimal processes at the microscopic level, thereby correctly capturing the kinematic features of the new physics model.

The simplified model framework for dark matter and dark sector searches at colliders should constitute a list of key relevant QFT interactions which first produce a mediator particle in a proton-proton collision which subsequently decays into other particles, including dark matter. In general such benchmark models would be characterised by the production mechanism (e.g. $q\bar{q}$ or gluon gluon, etc), the type of the mediator (e.g. scalar, pseudo-scalar, vector or axial-vector) and the decay channel (e.g. s-channel or t-channel production of two dark matter fermions, or other DM particle species). Secondly, each individual class of these simple models should be characterised by an appropriately chosen minimal set of physically relevant parameters (coupling constants, masses and widths).

The uses of the simplified model approach in the context of mono-jets and mono-photons searches at colliders and the discussion of its scope have become particularly relevant now in the light of the forthcoming run 2 of the LHC. The emerging framework is attracting a fair amount of attention in the collider and phenomenology communities. Two recent overviews [2, 3] give an example of this. The aim of the present paper is to go beyond the Born-level processes of dark matter production in the quark-anti-quark channel and include processes with gluons in the initial state.

The authors of Ref. [2] have discussed examples of tree-level benchmark processes relevant for interpreting DM searches at colliders, specifically: quark-anti-quark s-channel processes mediated by Scalar $(\mathrm{S})^{s}_{q\bar{q}}$ and Vector $(\mathrm{V})^{s}_{q\bar{q}}$ messengers; and the t-channel processes mediated by Colored Scalar $(\mathrm{CS})^{t}_{q\bar{q}}$ messengers. They have also considered gluon fusion via dimension-5 EFT operators mediated by Scalar $(\mathrm{S})^{\mathrm{EFT}}_{gg}$ and Pseudo-scalar messengers $(\mathrm{P})^{\mathrm{EFT}}_{gg}$ and have commented on EFT models in which DM coupled preferentially to the third generation.

We will extend these considerations by computing gluon fusion processes at 1-loop-level in a microscopic theory and apply this analysis to simplified DM models with scalar (S) and pseudo-scalar (P) mediators. To enable a direct comparison between models with different mediator types for the LHC reach, we will also re-evaluate the predictions of vector (V) and axial-vector (A) mediators produced in the quark-anti-quark channel.

Our work is also complimentary to the recent White Paper [3] which has concentrated specifically on the cases of vector and axial-vector messengers in the $q\bar{q}$ channel. More generally, i.e. going beyond the point of which specific mediator-types are included, Ref. [3] has addressed an important task of identifying the minimal number of relevant parameters characterising simplified models for DM collider searches. Their proposal is to select four parameters: the DM mass $m_{\rm DM}$, the mediator mass $m_{\rm MED}$, and the two coupling constants: $g_{\rm SM}$ characterising the coupling of the SM quarks to the mediator, and $g_{\rm DM}$ which is the coupling of the mediator to dark particles.

We would like to emphasise here the importance of the mediator width $\Gamma_{\rm MED}$ which we will treat as an independent parameter inherent in the characterisation of the simplified models. The impact of $\Gamma_{\rm MED}$ in mono-jet searches has been already discussed in earlier literature, see e.g. [4, 5, 7–9]. The DM production cross section at colliders scales numerically as $\sigma \propto g_{\rm SM}^2 g_{\rm DM}^2/(m_{\rm MED}^4 \Gamma_{\rm MED})$, i.e. inversely proportional to the width, leading to a resonant enhancement of the cross section at small values of $\Gamma_{\rm MED}$ as pointed out in [3].

In the approach of Refs. [3, 13] the messenger width was computed within the simplified model itself. But this assumes that the messenger can only decay into the DM particles as well as the $q\bar{q}$ pairs from which it was produced in the first place. This is a strong assumption which we are not prepared to apply universally, as this would exclude the possibility of mediators decaying into anything except a single species of the cosmologically stable DM within the dark sector (and would also limit the decay possibilities into SM particles). Instead, as already pointed out above, we will treat $\Gamma_{\rm MED}$ as a free parameter which we will vary and whose minimal value should not be less than the calculated width into DM and the appropriate SM channels[2]. We advocate the approach with four parameters: $m_{\rm MED}$, $\Gamma_{\rm MED}$, $m_{\rm DM}$ and the product of the couplings of the mediator to the SM and to DM particles, $g_{\rm eff}^2$. In order to provide a fully flexible Monte Carlo tool for experimental studies we have implemented the models described above in the MCFM framework [17–19]. The results of this paper extend the existing dark matter processes in MCFM [7], which focused primarily on NLO corrections in the effective field theory approach (matching to parton showers was achieved in ref. [20]. The results we present here will be available in the next public release of MCFM.

This paper is organised as follows. We first briefly discuss the limitations of the EFT approach at collider searches and proceed to define and setup the simplified models we study in Sec. II. In Section III we assemble the necessary formulae for DM scattering cross sections for our models relevant to direct detection and indirect detection of DM experiments. In Sec. IV we discuss the event generation and reconstruction as well as existing measurements for mono-jet final states, and proceed to present limits and projections for our simplified models. Following this, in Sec. V we extend our simplified models to allow for the possibility of additional contributions of new very heavy particles to the mediator production mechanism from initial state gluons. In the Appendix for the convenience of the Reader we list the basic amplitudes for a scalar mediator plus jet production in the spinor helicity formalism. Our conclusions are presented in Sec. VI.

II. SIMPLIFIED MODELS

In this article we focus primarily on mono-jet searches, induced by a mediator interaction between gluons and dark particles. We stress here that collider limits apply whether the dark particles are dark matter candidates or not, i.e. no assumption on their cosmic abundance or astrophysical production mechanism is required.

The promising kinematics of the mono-jet signature [21–25] was appreciated for new physics searches several years ago [26–28, 31]. Models studied include those with extra-dimensions [32] to compressed SUSY spectra [33–35]. More recently it was also argued that this configuration can constrain dark sectors in a fairly model-independent way [5, 6, 29–31, 36, 37]. To limit the number of free parameters and to facilitate the interpretation and cross correlation of measurements at colliders and direct detection experiments effective operators were proposed to parametrise the signal hypotheses, i.e. the contributions of new physics models.

---

[2] Recently while this paper was being finalised, Ref. [14] appeared, considering scalar and pseudo-scalar mediators in the gluon fusion channel and also pointing out the importance of keeping the mediator width a free parameter. Limits for invisible decays of the Higgs boson in mono-jet measurements, taking the full top-mass dependence into account, have been obtained in recent years [15, 16].

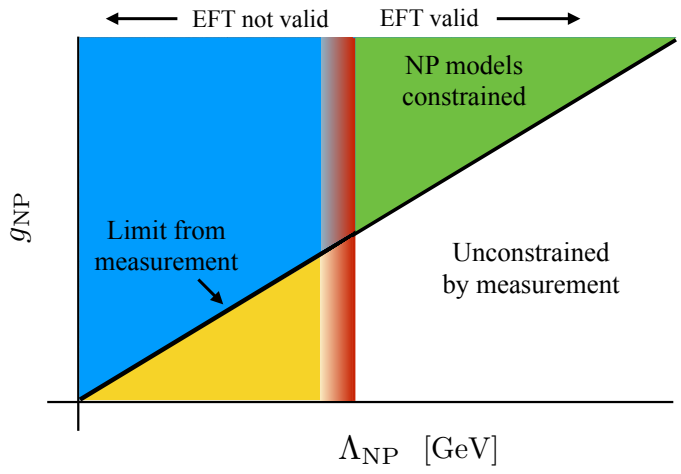

FIG. 2: Figure taken from [38], schematically illustrating the valid interpretations of experimental results in terms of EFTs. Experimental analyses set a bound on the g_{NP}/Λ, corresponding the solid line, combinations of g_{NP} and Λ greater than this bound are excluded. However, if the experiment was able to probe the scale of the new physics then the EFT prescription was invalid, this corresponds to all values left of the vertical line.

A priori, following the discussion in [38], the use of effective operators in constraining new physics scenarios in a fairly model independent way is a legitimate approach in parts of the model parameter space. Differential distributions can always be used to constrain the Wilson coefficients C_i of specific effective operators O_i. It needs to be kept in mind, however, that these constraints are only meaningful when the scale at which the operators are probed is below the validity region of the effective theory, e.g. $\sqrt{\hat{s}} \ll \Lambda_{\rm NP}$. This constraint results in the red vertical line of Fig. 2. Because $C_i \sim g_{\rm NP}/\Lambda_{\rm NP}$, a constraint from a measurement on the Wilson coefficient translates into a diagonal curve depicted in black in Fig. 2, resulting in four regions of the parameter space of new physics models. While the sectors left of the vertical red line are outside the validity range of the effective theory, only the models that fall into the green region could be constrained by the measurement. More specifically, when aiming for an interpretation of the constraint on the effective operator in terms of a new physics model, models that are constrained have to have a high new physics scale, i.e. $\sqrt{\hat{s}} < \Lambda_{\rm NP} \simeq m_{\rm NP}$, and a large coupling $g_{\rm NP}$. This can require the dark particles to be strongly coupled to the visible sector, which further complicates the interpretation.

Therefore, a reliable interpretation of collider searches of dark matter particles should be based on basic QFT interactions where all intermediate propagating degrees of freedom in a given process are explicitly taken into account[2, 39–42] Unsurprisingly, contributions due to light degrees of freedom have been found to be significant for limit setting [4, 7, 9–12].

In order to model mediator production, we will consider simplified models with the mediators to the dark sector associated with scalar S, pseudo-scalar P, vector Z' and axial-vector Z'' fields with interactions,

$$\mathcal{L}_{\rm scalar} \supset -\frac{1}{2}m^2_{\rm MED}S^2 - g_{\rm DM}S\,\bar{\chi}\chi - g^t_{SM}S\,\bar{t}t - g^b_{SM}S\,\bar{b}b\,, \tag{1}$$

$$\mathcal{L}_{\rm pseudo-scalar} \supset -\frac{1}{2}m^2_{\rm MED}P^2 - g_{\rm DM}P\,\bar{\chi}\gamma^5\chi - g^t_{SM}P\,\bar{t}\gamma^5 t - g^b_{SM}P\,\bar{b}\gamma^5 b\,, \tag{2}$$

$$\mathcal{L}_{\rm vector} \supset \frac{1}{2}m^2_{\rm MED}Z'_\mu Z'^\mu - g_{\rm DM}Z'_\mu\bar{\chi}\gamma^\mu\chi - \sum_q g^q_{SM}Z'_\mu\bar{q}\gamma^\mu q\,, \tag{3}$$

$$\mathcal{L}_{\rm axial} \supset \frac{1}{2}m^2_{\rm MED}Z''_\mu Z''^\mu - g_{\rm DM}Z''_\mu\bar{\chi}\gamma^\mu\gamma^5\chi - \sum_q g^q_{SM}Z''_\mu\bar{q}\gamma^\mu\gamma^5 q\,. \tag{4}$$

Two types of coupling constants appear in these equations: $g_{\rm SM}$ which collectively denote the couplings between messenger fields and Standard Model particles, and $g_{\rm DM}$ which are couplings of the messenger to the dark sector χ particles. We have assumed that the scalar and pseudo-scalar messengers are coupled only to top and bottom

quarks with the Yukawa-type coupling denoted $g_{SM}^{t,b}$ in Eqs. (1)-(2) – these are the dominant interactions of (pseudo)-scalars with the SM fermions; in fact in most cases only the couplings to tops are important. Phenomenologically this resembles models with minimal flavour violation [43] and a SM-Yukawa-like hierarchy for the mediator-fermion interactions. The couplings of messengers to all six flavours of SM quarks are taken to be proportional to the corresponding Higgs Yukawa couplings, y_q, and to make our definitions look symmetric we choose to parametrise the DM couplings in a similar fashion, so that,

$$\text{for scalar \& pseudo} - \text{scalar messengers}: \quad g_{\rm SM}^q \equiv g_q y_q\,, \quad g_{\rm DM} \equiv g_\chi y_\chi\,, \quad \text{where} \quad y_\chi \equiv \frac{m_\chi}{v} = \frac{m_{\rm DM}}{v}\,. \tag{5}$$

The product of the top and χ couplings to messengers is,

$$g_{\rm eff}^2 \;:=\; g_{\rm SM}^q\, g_{\rm DM} \;=\; g_t g_\chi\, y_t y_\chi \;=\; g_q g_\chi\, \frac{m_t m_{\rm DM}}{v^2}\,, \tag{6}$$

and we keep the scaling g_q flavour-universal for all quarks, so $g_t = g_q$.

All vectors and axial-vectors are assumed to be coupled to all quarks uniformly, hence the sums in Eqs. (3)-(4) are over all quark flavours (with a universal gauge-type coupling denoted $g_{\rm SM}$). For the axial-vector and vector mediators we will use

$$g_{\rm eff}^2 \;:=\; g_{\rm SM}\, g_{\rm DM}\,. \tag{7}$$

In our setup the Standard Model particles only interact via the mediator with the invisible sector, i.e. the particle χ. Thus, all amplitudes contributing to the processes we will study in Secs. III-V are proportional to $g_{\rm eff}^2$ defined in Eqs. (6) and (7).

It is important to stress that models derived from scalar and pseudo-scalar mediators provide some of the simplest realisations of a non-minimal Higgs sector in which the Standard Model Higgs interacts and can mix with the scalar mediators. Following the Higgs discovery there is a renewed interest in the literature in Higgs portal models where the scalar mediators are SM-singlets but the SM Higgs h interacts with them via the interaction, $\lambda_{\rm hp}|H|^2|\Phi|^2$. The Higgs portal models with singlet scalar messengers will be treated in the same way as general scalar messengers. These models provide a direct link with Higgs physics and also include theoretical scenarios which manifest a common origin of the electroweak and the DM scales in Nature as was recently explored in Refs. [44–53].

More specifically, consider the case where the mediator is a complex scalar Φ which is a singlet of the SM and interacts with it only via the portal interactions with the Higgs,

$$\mathcal{L}_{\rm portal} = \lambda_{\rm hp}|H|^2|\Phi|^2 - g_{\rm DM}\ \bar{\chi}\Phi\chi. \tag{8}$$

Furthermore, we assume that Φ is charged under the gauge group of the dark sector and is coupled to other dark particles (which in (8) for simplicity are taken to be the dark fermions χ and $\bar{\chi}$, but this can be extended to include vector and scalar dark particles). In models which contain no input mass scales in the microscopic Lagrangian, the vacuum expectation value for the field Φ can be generated quantum mechanically, e.g via the Coleman-Weinberg mechanism [54] in the dark sector as explained in [44]. The VEV $\langle\Phi\rangle$ then induces the vacuum expectation value v for the Higgs field via the portal interaction in Eq. (8) and triggers electroweak symmetry breaking. It also generates the mass scale $m_{DM} = g_{\rm DM}\ \langle\Phi\rangle$ in the dark sector. Thus, in this class of models the electroweak scale and dark matter scale have a common origin. To see that such Higgs portal models continue to be described effectively by the minimal simplified model in Eq. (1) we re-write (8) after electroweak symmetry breaking, in unitary gauge, as,

$$\mathcal{L}_{\rm portal} \supset 2\lambda_{\rm hp}\,\langle\Phi\rangle\, v\ \phi h + \lambda_{\rm hp} v^2\ \phi^2 + \lambda_{\rm hp}\,\langle\Phi\rangle^2\, h^2 - g_{\rm DM}\ \bar{\chi}(\langle\Phi\rangle + \phi)\chi. \tag{9}$$

Transforming into the mass eigenstate basis, we find two scalar resonances h_1 and h_2, both of which interact with the Standard Model and the dark sector. Either state can be identified with S in Eq. (1).[3]

Following a similar line of reasoning for the case where the pseudo-scalar can develop a vev and CP is not a good quantum number we can map the Higgs portal interactions to the form of Eq. (2).

We note that the scalar and pseudo scalar Lagrangians defined above are compatible with the principle of minimal flavor violation. If on the other hand one were to relax this constraint one could define a scalar (and pseudo-scalar)

---

[3] For simplicity and concreteness, this paper concentrates on the simplified models with mediators coupled to Dirac fermions χ in the dark sector. These models can be extended to incorporate scalar and vector dark matter particles as in [46–48] and chiral fermions.

Lagrangian in which the mediating particle couples directly to the light quark species, with no Yukawa suppression. In these instances the phenomenology of the signal changes substantially, since the production mechanism is now identical to vector and axial-vector mediators. As a result the phenomenology of these signatures, (LHC limits and cross sections) are similar in size to those obtained using the vector and axial mediators (the major differences arising from a scalar mediator is an isotropic final state with no spin correlations). We note that these processes are available in MCFM [7], and the analysis we present here could be applied easily to these models, however for brevity we do not consider them in this paper.

A. The mediator width

We would now like to discuss the impact of the mediator width in our simplified models. Given the models specified in Eqs. (1)-(4) with democratic quark-(axial)vector and Yukawa-type quark-scalar interactions we obtain a lower limit for the width of the mediator. For scalar and pseudo-scalar mediators, depending on their mass, decays to heavy quarks may or may not be open (i.e. $m_{\rm MED}$ is required to be $> 2m_t$ for an open decay). In certain regions of parameter space, loop induced decays to vector bosons, or extended dark sector decays, and off-shell decays (e.g. to $t^*\bar{t}$), may significantly enhance the "minimal widths" which we define as,

$$\Gamma^{V,A}_{\rm MED,min} = \Gamma^{V,A}_{\chi\overline{\chi}} + \sum_{i=1}^{N_f} N_c \Gamma^{V,A}_{q_i\bar{q}_i} + N_c \Gamma^{V,A}_{t\bar{t}} \tag{10}$$

$$\Gamma^{S,P}_{\rm MED,min} = \Gamma^{S,P}_{\chi\overline{\chi}} + N_c \Gamma^{S,P}_{t\bar{t}} \tag{11}$$

where $\Gamma_{\chi\overline{\chi}}$ is the mediator decay rate into two DM particles (which here we assume are fermions $\chi\overline{\chi}$, modifications to scalar dark matter are trivial to incorporate). The sum on the right hand side of the first equation is over the massless SM quark flavours interacting with the vector and axial-vector mediators. These widths are lower bounds on the total and as such we treat the width as a free parameter and investigate the LHC phenomenology as a function of the rescaled width. For decays into fermions the partial widths are defined as follows,

$$\Gamma^{V}_{f\overline{f}} = \frac{g_f^2(m^2_{\rm MED}+2m_f^2)}{12\pi m_{\rm MED}}\sqrt{1-\frac{4m_f^2}{m^2_{\rm MED}}} \tag{12}$$

$$\Gamma^{A}_{f\overline{f}} = \frac{g_f^2(m^2_{\rm MED}-4m_f^2)}{12\pi m_{\rm MED}}\sqrt{1-\frac{4m_f^2}{m^2_{\rm MED}}} \tag{13}$$

$$\Gamma^{S}_{f\overline{f}} = \frac{g_f^2 m_f^2 m_{\rm MED}}{8\pi v^2}\left(1-\frac{4m_f^2}{m^2_{\rm MED}}\right)^{\frac{3}{2}} \tag{14}$$

$$\Gamma^{P}_{f\overline{f}} = \frac{g_f^2 m_f^2 m_{\rm MED}}{8\pi v^2}\left(1-\frac{4m_f^2}{m^2_{\rm MED}}\right)^{\frac{1}{2}} \tag{15}$$

where m_f denotes masses of either SM quarks q or DM fermions χ and the coupling constant g_f denotes either g_q or g_χ as defined on the right hand side of Eq. (5). In Fig. 3 we plot the minimal widths computed using Eqs. (10)-(15) for scalar and vector types of the mediators as functions of the mediator mass, for two representative choices of DM masses. As expected, the (pseudo)-scalar models parameterised in terms of Yukawa couplings, are much more sensitive to the choice of DM mass. The hadronic branching ratio for the vector mediator dominates the decays (due to the combination of light flavours and color factors $N_f N_c$), extended darks sectors could result in larger branching ratios to the dark sector and thus increase the width. For the scalar there are no light decays (apart from $b\bar{b}$ which can become important for light mediators), and the relative enhancement/suppression of $t\bar{t}$ decays scales like $N_c(m_t/m_{DM})^2$.

In summary: The set of simplified models for dark particle searches we study is defined by Eqs. (1)-(4). It automatically accounts for Higgs portal models with scalar and pseudo-scalar messengers. In Sec. V we will further extend the model in Eq. (1) by adding a new BSM interaction (21).

Our simplified models are characterised by the type of the mediator field, which can be a scalar, pseudo-scalar, vector or axial-vector particle. There are four (five) types of input parameters involved in this description: the mediator

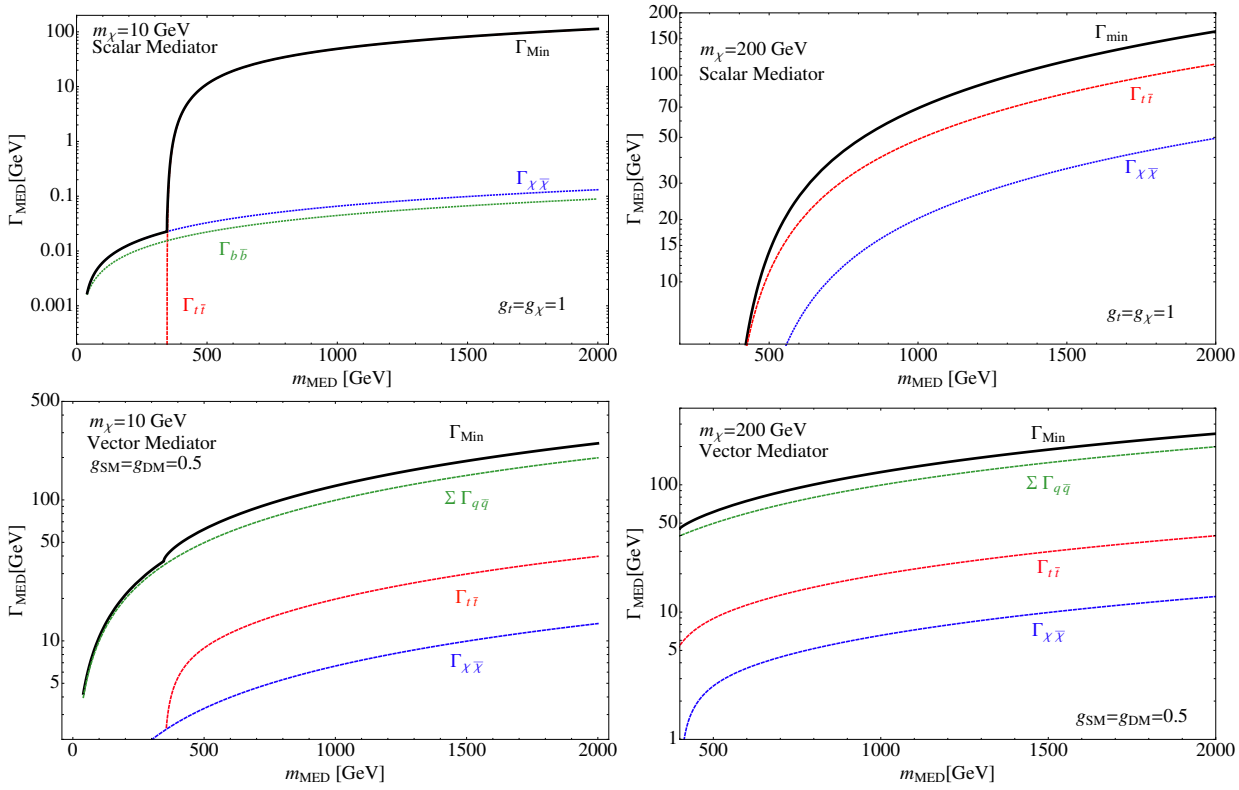

FIG. 3: Minimal width as a function of the mediator mass for scalar and vector operators, with two different DM mass choices. Individual partial width contributions are illustrated.

mass $m_{\rm DM}$, the mediator width $\Gamma_{\rm DM}$, the dark particle mass $m_{\rm DM}$ and an appropriately defined coupling constant (or constants) to characterise the combined effect of the SM-mediator and the mediator-Dark sector interaction.

We use $g_{\rm SM}\, g_{\rm DM}$ as the input effective coupling parameter for the vector and axial-vector cases (3)-(4). In the cases of scalar and pseudo-scalar mediators (1)-(2) we choose to scale the couplings with the SM Yukawa's and use the product of scaling factors $g_q\, g_\chi$ defined in (5) as the input effective coupling parameter.[4] (The extended model studied in Sec. V will contain an additional coupling g_g.)

III. DIRECT AND INDIRECT DETECTION LIMITS

If we make the assumption that the particle χ of Eqs. (1)-(4) is a dark matter candidate, accounting for the observed dark matter abundance in the universe, we can derive limits on our simplified models from low-energy interactions, i.e. direct and indirect detection experiments. Direct detection experiments measure the recoil of the nucleus of which the dark matter particle scatters off. Our limits are based on measurements by LUX [55–57] which currently provides the strongest bounds for $m_{\rm DM} \gtrsim 6$ GeV. In these settings dark matter particles are assumed to be non-relativistic, the momentum transfer (depicted in the right diagram of Fig. 1) is small and describing the interaction in terms of effective operators is justified as long as $\mathcal{O}(m_{\rm MED}) \gtrsim 1$ GeV.

For the calculation of the scattering cross section of a dark matter particle scattering spin-independently via a

[4] The choice of what is treated as the input coupling parameter for (pseudo)-scalar mediators, namely the combination $(g_{\rm SM}/y_q)(g_{\rm DM}/y_\chi)$, or $(g_{\rm SM}/y_q)g_{\rm DM}$, or the original couplings $g_{\rm SM}\, g_{\rm DM}$ is of course only a simple re-parametrisation which only affects which dimensionless parameters are held fixed when one varies the mass parameters for the mediators/dark particles in the plots. We have chosen the first combination, the authors of [14] used the second, while the vector cases of course have no Yukawa's to scale. In any case this is a simple re-parametrisation.

vector mediator off a proton we find

$$\sigma^V_{\chi \mathrm{p}} = \frac{9}{\pi} \frac{g^2_{\mathrm{DM}} g^2_{\mathrm{SM}} \rho^2}{m^4_{\mathrm{MED}}} \tag{16}$$

and for the scalar, interacting with the nuclei only via the gluons, we use [58–60]

$$\sigma^S_{\chi \mathrm{p}} = \frac{\rho^2}{\pi} \left| \frac{m_p}{m_t} \frac{g_t y_t}{m^2_{\mathrm{MED}}} \frac{g_\chi y_\chi}{} \frac{2}{27} f_{\mathrm{TG}} \right|^2, \tag{17}$$

where $\rho = m_{\mathrm{DM}} m_p/(m_{\mathrm{DM}} + m_p)$ is the reduced mass and $f_{\mathrm{TG}} \simeq 0.9$ [61].

Axial-vector mediators result in spin-dependent dark matter-proton scatterings, with the cross section described by [62]

$$\sigma^A_{\chi \mathrm{p}} = \frac{3}{\pi} \frac{g^2_{\mathrm{DM}} g^2_{\mathrm{SM}} a^2 \rho^2}{m^4_{\mathrm{MED}}}, \tag{18}$$

with $a = \Delta u + \Delta d + \Delta s \simeq 0.43$ [9, 61], assuming democratic couplings to all quark flavors. We compare the predicted cross sections with the combined bounds of Wimp-proton-scattering limits of PICASSO [63], COUPP [64] and SIMPLE [65].

While direct detection experiments can give strong constraints for the vectors and the scalar mediator, the scattering of a pseudo-scalar off a nucleus is strongly velocity dependent and vanishes in the non-relativistic limit. Therefore, for pseudo-scalars, taking existing limits into account [66, 67], indirect detection experiments can result in stronger bounds than direct detection experiments [68, 69]. For the simplified model of Eq. (2), using the s-wave velocity-averaged DM annihilation cross section into $\bar{b}b$,

$$\langle \sigma v \rangle^P_{\bar{b}b} = \frac{N_C}{2\pi} \frac{(y_b g_b)^2 (y_\chi g_\chi)^2 \, m^2_{\mathrm{DM}}}{(m^2_{\mathrm{MED}} - 4 m^2_{\mathrm{DM}})^2 + m^2_{\mathrm{MED}} \Gamma^2_{\mathrm{MED}}} \sqrt{1 - \frac{m^2_b}{m^2_{DM}}}, \tag{19}$$

we can derive a bound on the parameters in the $\bar{b}b$ channel [66]. As always, the scaling factors g_q are kept flavour-universal, so $g_b = g_t = g_q$ in these equations.

In all four expressions for the cross sections (16)-(19) for scalar and pseudo-scalar mediators we will keep g_q and g_χ fixed, while for vector and axial-vector mediators we fix g_{SM} and g_{DM}.

IV. SEARCHES AT THE LHC

A. Event generation and final state reconstruction

We generate the processes $pp \to (X \to \bar{\chi}\chi)$+jet where X can be a vector, axial-vector, scalar or pseudo-scalar using MCFM. The existing implementation of DM process in MCFM (described in ref. [7]) consisted of NLO predictions for vector, axial-vector, scalar and pseudo-scalar mediators in the effective field theory prescription, in addition LO processes involving a scalar mediator and top quark loop were also included. In the previous version propagating resonances were included for the above process in an *ad hoc* manner in which the user specified the value of the width, mediator mass and couplings, in addition to the mass of the dark matter particle. We have extended the code to include the LO process in which a pseudo scalar mediator couples to the top quark loop, and parameterized the code in terms of the simplified models described in the previous section. In addition we have included heavy new physics in the loop for scalar and pseudo-scalar mediator, but we postpone discussion of these effects to the next section. These extensions to the code will be released publicly in the next version of MCFM.

The generated signal samples are showered using Pythia 8 [70] with tune 4C. The background yield for our 8 TeV limits are entirely inferred from the CMS mono-jet searches [24]. To emulate the detector performance the showered samples are clustered using the anti-k_T [71] algorithm with a cone size of 0.4. The resulting three leading jets with a p_T above 15 GeV are smeared following the resolution functions quoted by CMS [72]. The remaining hadronic recoil is smeared following the MET resolution quoted in [73].

For the 14 TeV analysis, the two leading backgrounds ($Z \to \nu\nu$ and $W \to \ell\nu$) are generated using MadGraph [74] and are smeared according to the same scheme discussed in the previous paragraph. From these samples a kinematic

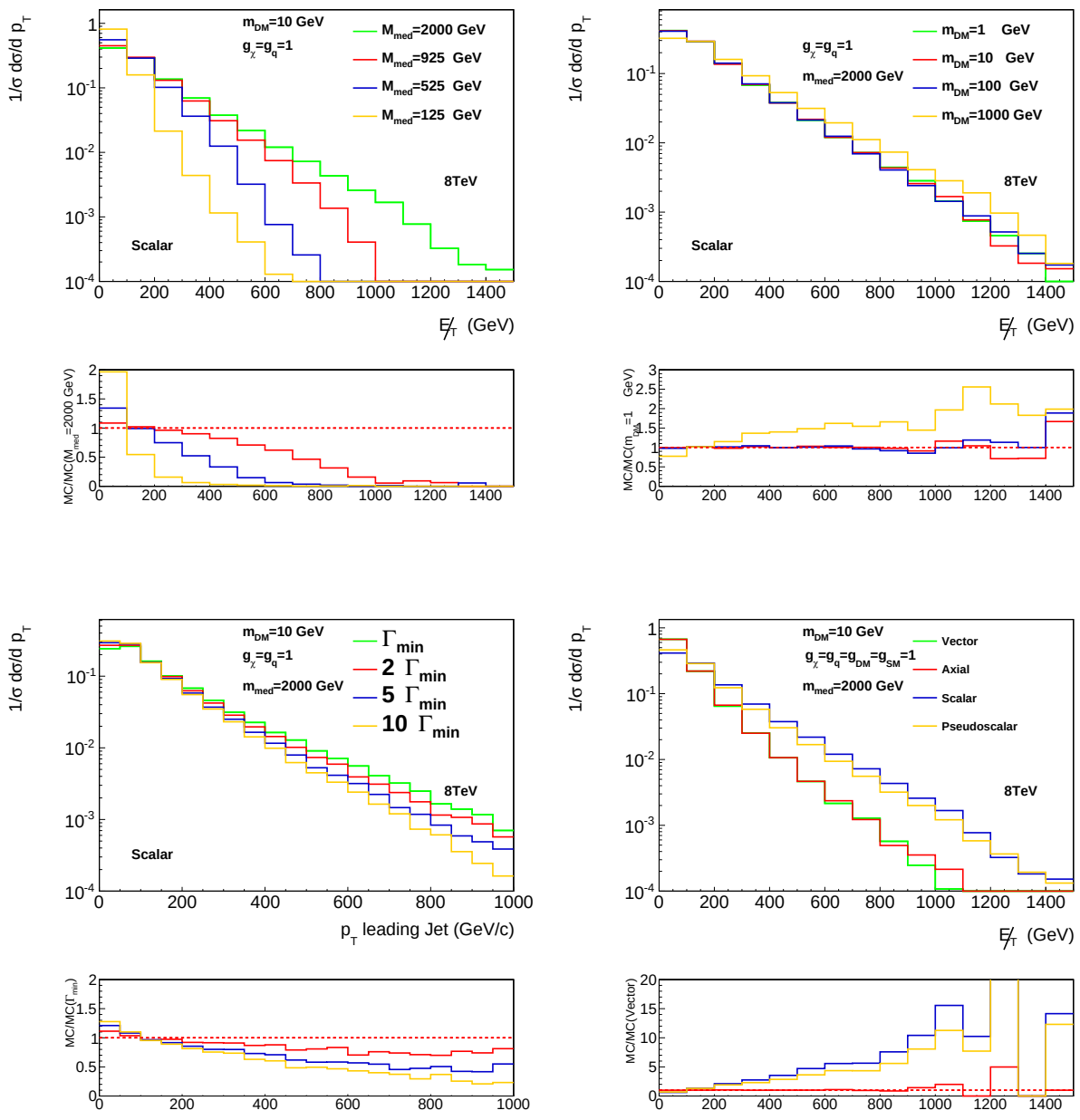

FIG. 4: Kinematics and reconstruction of selected distributions. Events are generated using MCFM and PYTHIA, detector level effects are also simulated. Plots are normalised to have the same yield so that kinematic differences can be observed. We set the coupling parameters defined in Eq. (5) to $g_\chi = 1 = g_q$ for (pseudo)-scalars and $g_{\rm DM} = 1 = g_{\rm SM}$ for (axial)-vector mediators.

scale factor is obtained. The cross-sections for all other process, excluding the $t\bar{b}$ and single top, are obtained by scaling the 8 TeV predictions in the CMS analysis by the NLO scale factor from 8 TeV to 14 TeV obtained in MCFM [18]. For the top and $t\bar{t}$ backgrounds the partial NNLO cross sections are used [75].

To be able to re-interpret the CMS mono-jet search in terms of the simplified models of Eqs. (1)-(4) we follow the event selection of [24] closely. The signal extraction region requires a $E_{\rm T}^{\rm miss} > 200$ GeV, which is beyond the plateau efficiency and thus, very close to 100%. The hardest jet in the event must fulfill $p_{T,j_1} \geq 110$ GeV and $|\eta| < 2.4$. We accept events with a second jet if $p_{T,j_2} \geq 30$ GeV, $|\eta| < 5.0$ and provided the azimuthal angle between the two jets is less than 1.8 radiants, i.e. $\Delta\phi_{j_1,j_2} < 1.8$. We veto events with more than two jets. To optimise the sensitivity of the analysis with respect to varying dark matter and mediator masses, the exclusion limits are based on 7 phase space regions distinguished by $E_{\rm T}^{\rm miss} > (250,\ 300,\ 350,\ 400,\ 450,\ 500,\ 550)$ GeV.

The limits shown in this section are based on the most sensitive of the 7 regions respectively. For each signal model, the 7 regions are scanned taking the most sensitive result obtained by scanning the individual regions. The limit computation is preformed in the same manner as that in the CMS analysis, profiling the likelihood and obtaining the 90% confidence level using the CL_S procedure. Both the systematics and statistical uncertainties as described in the CMS mono-jet analysis are taken into account. As a cross check, the cross section limit results were reproduced to within 3%. For 14 TeV we use the same reconstruction approach, keeping the same systematics, but scaling the yields by the predicted scale factors.

In Fig. 4 we present a series of differential distributions obtained using the prescription defined above, focusing primarily on the case of a scalar mediator. Most of the kinematic properties can be inferred from the on-shell condition for the mediator, namely

$$(\not{E}_T^{min})^2 + 4m_{DM}^2 < s_{\chi\overline{\chi}} \sim M_X^2 \tag{20}$$

As the mediator particle becomes heavier the missing transverse energy spectrum becomes harder, as illustrated by the top left plot in Fig. 4. The lower left plot in Fig. 4 illustrates the jet p_T dependence on the width. Broader widths result in a spreading of $s_{\chi\overline{\chi}}$, however events which become more energetic are additionally damped by PDF suppression. Therefore as particles acquire broader widths distributions are naturally softened relative to the narrow width case. Finally the lower right plot in Fig. 4 illustrates the differences in the MET spectrum associated with the production mechanism, the gluon induced scalar and pseudo scalar processes result in a harder spectrum.

Small kinematic differences are observed between each of the gluon induced processes or vector induced processes. The largest modifications to the kinematic shape come from variations in the mediator mass, and variation in the width. When scanning the dark matter mass, visible modifications of the kinematics shapes are only present for off-shell masses.

B. Experimental Searches

In Figure 5 we plot the limits on the LHC cross section at 8 TeV and projected limits at 14 TeV for scalar, pseudo-scalar, vector and axial-vector mediators, as the function of the mediator mass. For the χ-particle dark matter mass we have chosen a relatively small value of 10 GeV, although the results obtained for heavier dark matter were found to be similar. The kinematics of the process is then completely specified once a coupling is set, since this fixes the minimal width of the mediator. For the coupling parameters we choose $g_g = g_\chi = 1$ in the scalar and pseudo-scalar case, and $g_{SM} = g_{DM} = 0.5$ for (axial)-vectors. With the kinematics of the model fixed the properties of the model allow a limit on a cross section to be derived. From the derived limit, a value, μ, is obtained which refers to the ratio of excluded cross section with respect to the predicted cross section as determined by the couplings and width constraint. Translating the constraint on μ to direct constraints on the couplings, g, requires propagating the cross section dependence of both the couplings and the width. Values with $\mu < 1$ typically indicate the excluded couplings and width are smaller than the tested model.

In each plot we show the exclusion contours for different choices of the mediator width $\Gamma_{\rm MED}$ starting with the minimal width $\Gamma_{\rm min}$ computed in each model for the given choice of parameters, and then scaling it upwards as $2 \times \Gamma_{\rm min}$, $5 \times \Gamma_{\rm min}$ and $10 \times \Gamma_{\rm min}$. We quote this both in terms of a cross section limit, and μ. For low values of the mediator mass, we find that an exclusion of order unity in μ. Additionally, we observe that increasing the energy from 8 to 14 TeV results in a sizable increase in the limit for heavy (> 1 TeV) mediators.

In order to obtain relevant exclusion limits for our simplified models, we must compare the predicted value of the cross section for a given parameter set against the limit set by the LHC (e.g. in Fig. 5). We present the constrained region as a function of the dark matter and mediator mass in Fig. 6.

To highlight the complementarity between the LHC limits and the direct detection (DD) experiments we present them on the same plots in Fig. 6. We stress, however, that the direct comparison between the collider limits on the production of a dark sector particle χ and the exclusion limits from direct detection and indirect detection dark matter experiments is only sensible for χ being the cosmologically stable DM. More generally, if χ is a representative of the dark sector and is only stable on collider time scales, but not cosmologically, DD and ID bounds are severely diluted relative to the LHC limits in Fig. 6, or even not applicable.

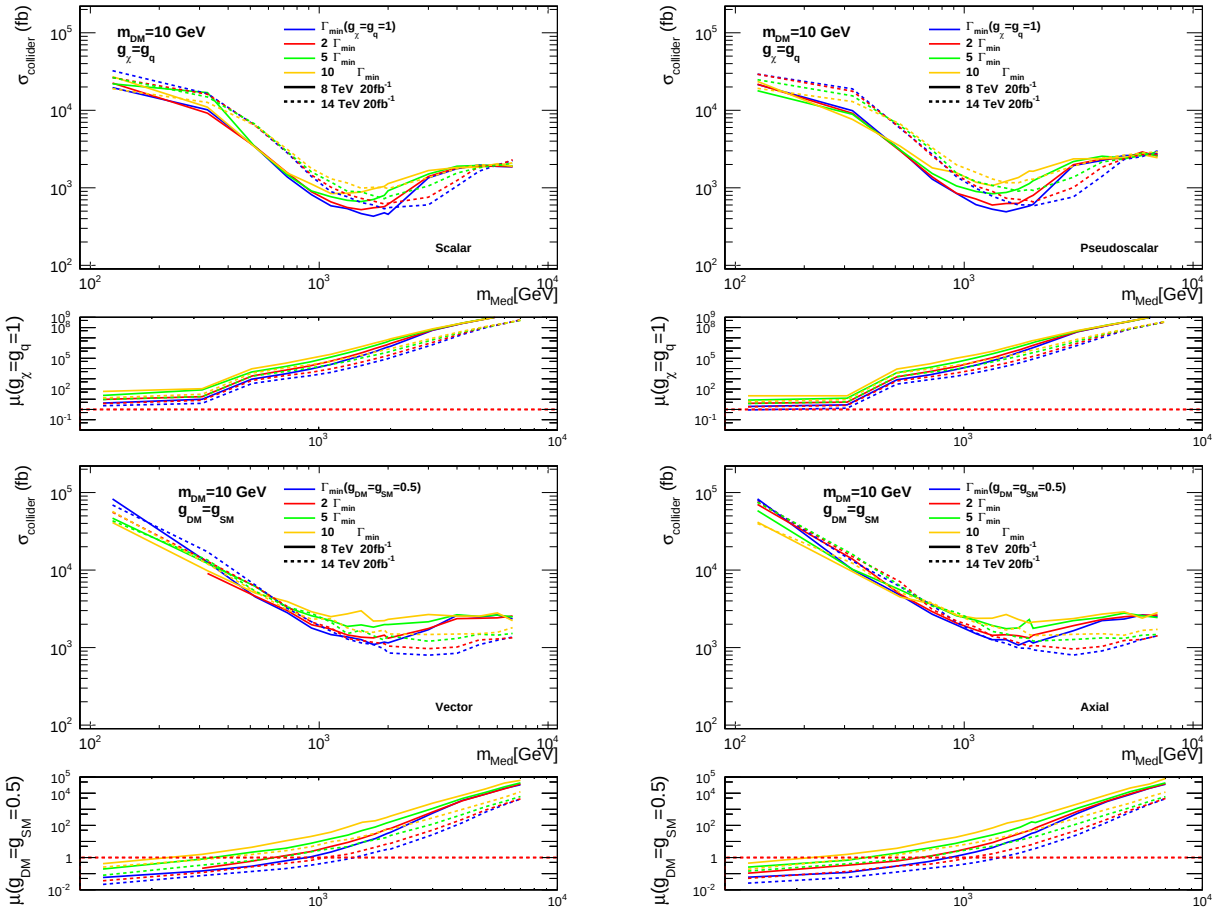

FIG. 5: Cross section limit bounds (projections) for LHC cross sections at 8 TeV (14) TeV for scalar (upper left), pseudo-scalar (upper right), vector (lower left) and axial vector (lower right). We chose $m_{DM} = 10$ GeV and set the coupling parameters defined in Eq. (5) to $g_\chi = 1 = g_q$ for (pseudo)-scalars and $g_{\rm DM} = 0.5 = g_{\rm SM}$ for (axial)-vector mediators. We also note that LHC exclusion bounds do not depend strongly on the dark matter mass, $\sigma_{collider}$ refers to the MCFM cross section for a parton $p_T > 15$ GeV.

We find that for our vector and axial-vector models described above, the LHC at 8 TeV can exclude mediator masses of < 1 TeV and dark matter masses of less than around 200 GeV. Our 14 TeV LHC at 20 fb^{-1} projection contours improve these, roughly speaking, by a factor of two. Note, however, that the collider limits are strongly dependent on the width of the mediator particle (due to the $\Gamma^{-1}_{\rm MED}$ scaling of the cross section), if the width is increased the limits become substantially weaker.[5] For direct detection experiments the limits for axial and vector are very different, which as is well established is due to the spin independent versus spin dependent nature of particular processes. For the spin independent vector scattering the direct detection experiments cover almost the entire available phase space in the plot (apart from very light DM < 5 GeV scenarios which fall below the threshold energy of the detector). On the other hand, spin-dependent interactions are not as strongly constrained by DD experiments, here constraints are strong for light mediators, but fall off quickly for heavier mediators. The complementarity of DD and collider experiments can scarcely be made more apparent then this plot illustrates.

Direct and indirect detection experiments are more constrained by the mediator mass than the dark matter mass (c.f. Eqs (16)-(19)), and as a result, are able to exclude a wider range of dark matter masses, at a cost of a smaller constraint on the mediator mass. For the scalar and pseudo-scalar case, no collider limit can be set with our choice of $g_\chi = g_q = 1$, that is to say, that experiments cannot presently exclude parameters arising from a model in which both couplings are exactly Higgs like (for $m_{DM} = 10$ GeV at least). From the lower panels of Fig. 5 it is clear

[5] Note that due to the shape of the LHC exclusions for different limits in Fig. 5, this is not a simple $\Gamma^{-1}_{\rm MED}$ relation.

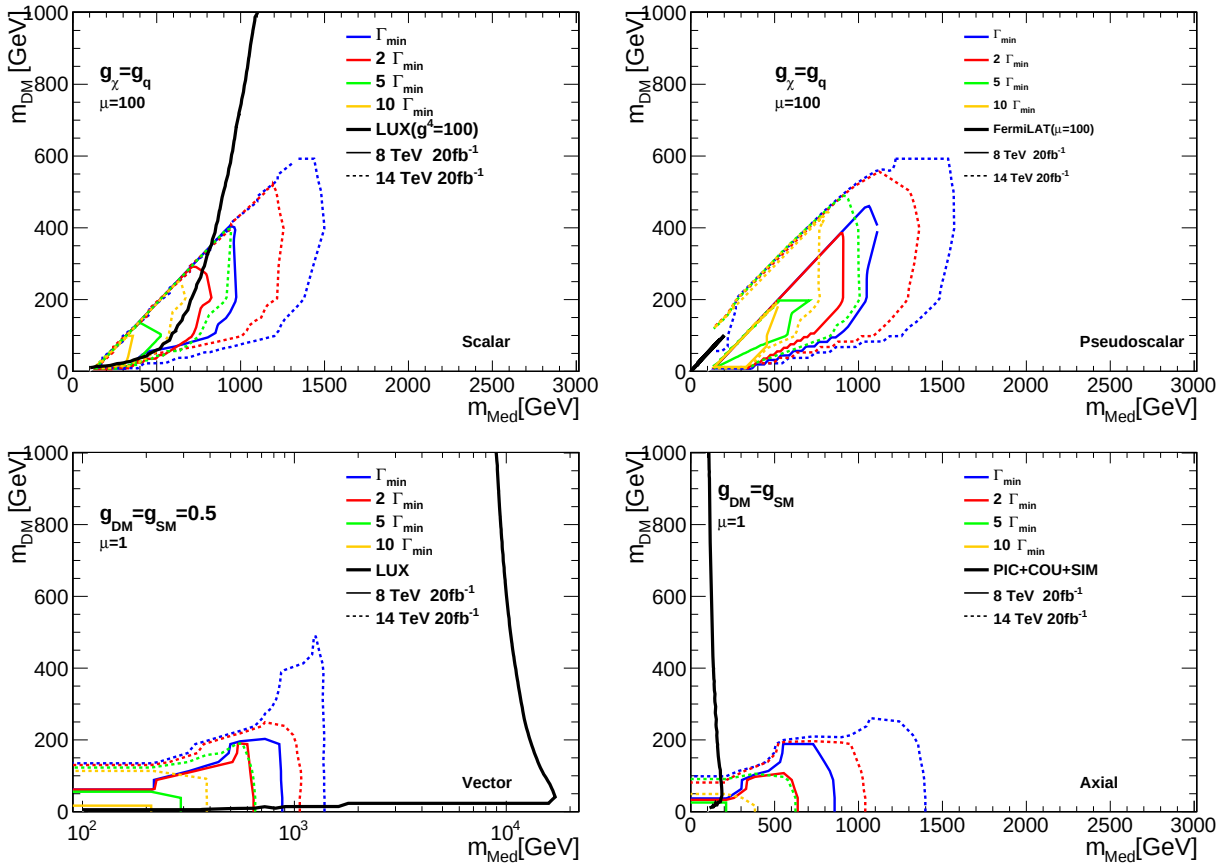

FIG. 6: $m_{\rm DM}$, $m_{\rm MED}$ exclusion planes for different potential mediators, for a variety of different mediator widths. We show the LHC 8 and the direct detection limits, in addition we present expected limits at LHC 14 TeV at 20 fb^{-1} as dotted lines. For scalar and pseudo-scalar mediators we increased the cross section by a factor of $\mu = 100$ as explained in the text. Data for direct detection results (in this and subsequent figures) comes from the LUX, [56], PICASSO [63], COUPP [64] and SIMPLE [65] experiments. For the pseudo-scalar mediator model on the top right plot we show the indirect detection limits using FERMI-LAT data [66].

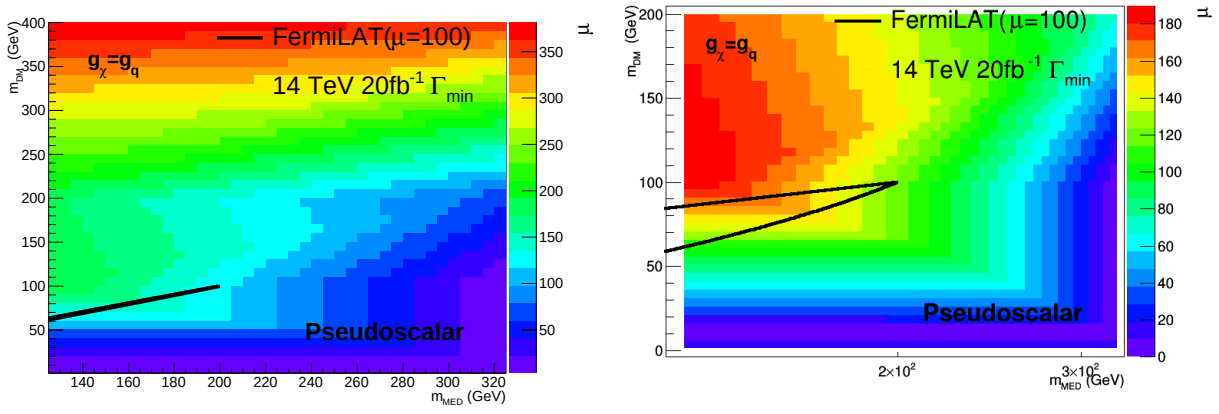

FIG. 7: Contour plots illustrating the signal enhancement μ-factor for pseudo-scalar mediator to achieve a 90% CL exclusion at 14 TeV LHC. The plot on the right shows exclusion contours for the low DM mass region, *cf.* top right plot in Fig. 6.

that if we increase the signal by a factor of $\mu = 100$ then limits can be derived. Note that this scale factor is not

completely unmotivated, the width of the mediator for scalar and pseudo-scalar mediators in our model is dominated by $t\bar{t}$ decays (in particular for light DM). Therefore increasing the cross section by a factor of 100 is approximately equivalent to changing $g_\chi \to 10 g_\chi$. Since we defined $g_{DM} = g_\chi m_{DM}/v$ increasing the coupling by a factor of 10 for light DM is completely plausible, for light dark matter, e.g. $m_{DM} \lesssim 25$ GeV , such that we remain well within the perturbative regime of $g_{DM} \lesssim 1$, and is basically equivalent to not requiring the mediator-χ interaction to scale like a Yukawa coupling. We note that the LUX and FERMI-LAT contours shown on the scalar and pseudo-scalar plots plot of Fig. 6 are obtained with the same rescaling, illustrating the challenge of searching for scalar mediators at all kinds of experiments. Extending the LHC reach to 14 TeV provides more stringent bounds, since the larger centre of mass energy allows heavier mediators to be probed.

Plots presented in Fig. 7 illustrate the contours of the required μ-factor necessary to enhance the signal for pseudo-scalar messenger models to set a 90% CL at 14 TeV LHC assuming the minimal width. The question of whether a parameter point is visible at the LHC depends on the ability to separate signal processes from the background. A better background rejection will boost sensitivity independently of the signal parameterisation and the real analysis sensitivity is likely to improve by a substantial amount. Hence this figure only serves as baseline for our current sensitivity. The plot on the right of Fig. 7 zooms into the relatively low DM mass region of the parameter space for pseudo-scalar mediators where the data from Indirect detection experiments become relevant.

Finally in Figs. 8 and 9 we show the plots in terms of the spin-dependent and the spin-independent DM–neutron cross sections for a more traditional comparison of collider limits in terms of our simplified models with the limits/projections from the direct and indirect detection experiments computed using cross section formulae in Sec. III. We compare the results in the $\sigma - m_{MED}$ and $\sigma - m_{DM}$ planes. The general pattern of Fig. 6 is reproduced, with

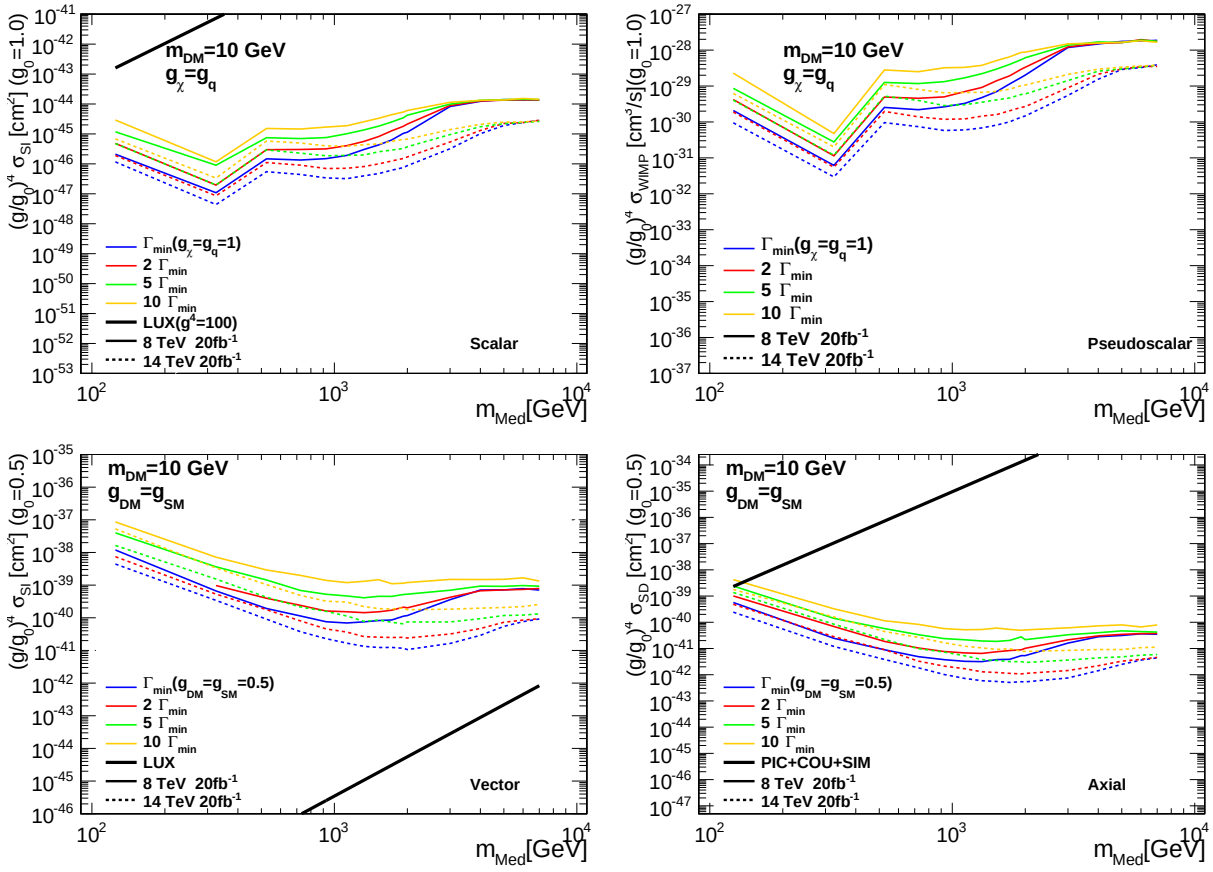

FIG. 8: Cross sections limits (projections) in terms of those reported by DD experiments, we show exclusions in terms of the spin-dependent and spin-independent cross sections against mediator mass for scalar, vector and axial-vector mediators. For the pseudo-scalar mediator we plot the DM pair annihilation cross-section. The corresponding limit from Indirect Detection experiments is too weak to show for the pseudo-scalar messenger.

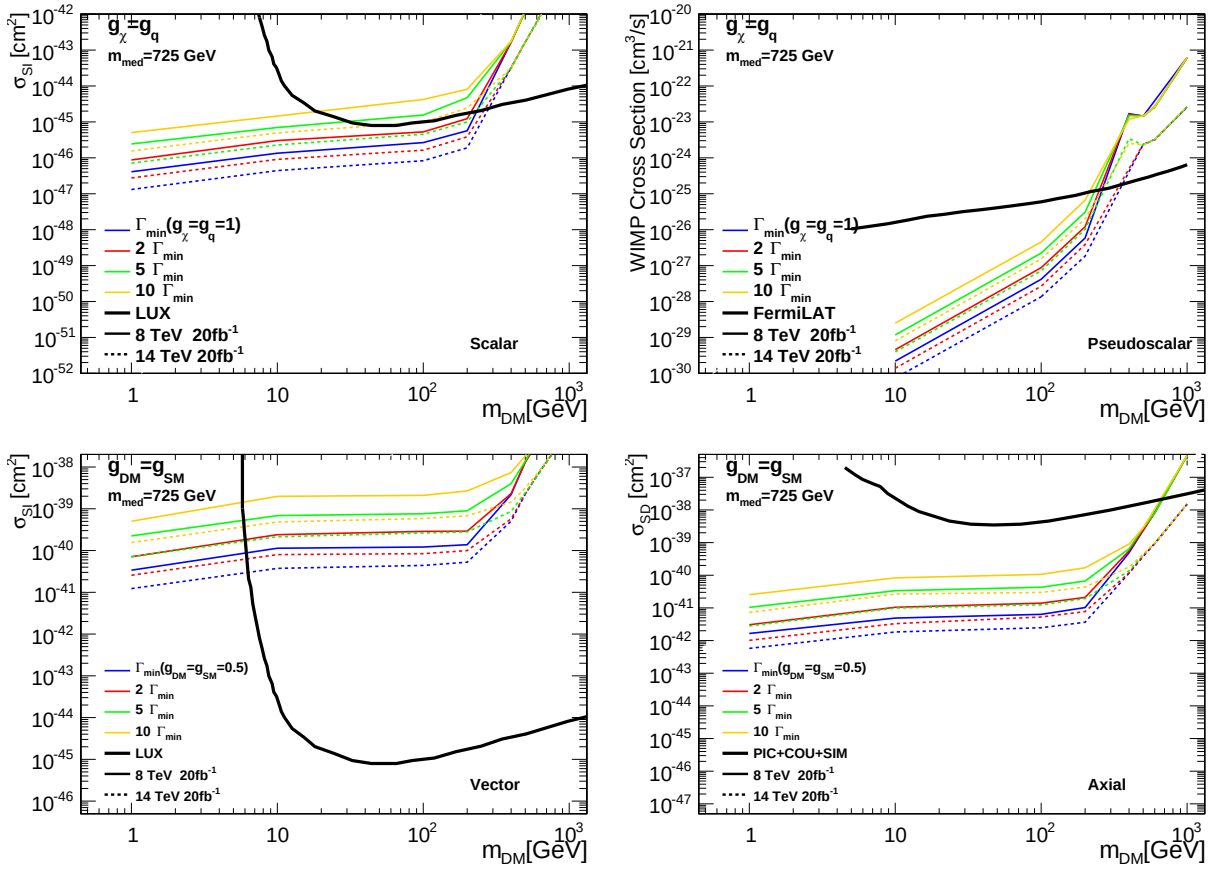

FIG. 9: Exclusion contours for the spin-dependent and spin-independent cross sections as in Fig. 8, now plotted as functions of the dark matter mass. For the pseudo-scalar mediator model we show the indirect detection limits (using FERMI-LATdata [66]). For the pseudo-scalar we show 95% C.L. exclusion limits, while we show limits at 90% C.L. for the other mediators.

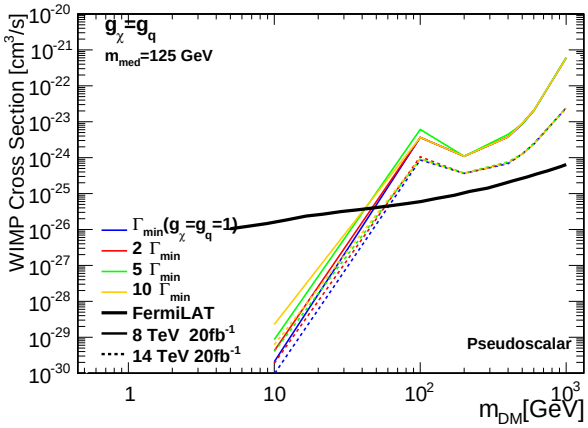

FIG. 10: The spin-independent cross section as in top right Fig. 9 for 125 GeV pseudo-scalar mediator mass.

spin-independent results from LUX providing the strongest bounds, for the axial and scalar cases the example we have chosen to illustrate is for a mediator which is too heavy to be efficiently probed at DD experiments, resulting in stronger bounds from the LHC.

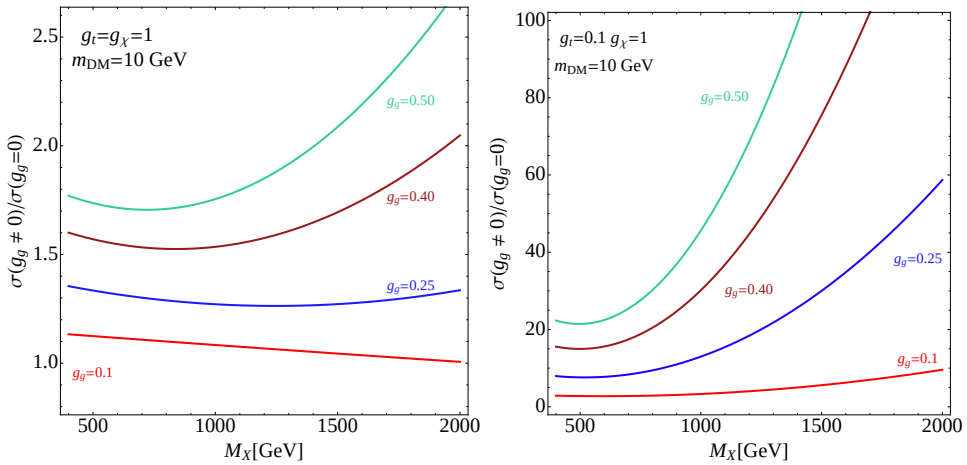

FIG. 11: Cross sections ratios describing the impact of the 5-dimensional contact interaction between gluons and the scalar mediator. The ratio is computed for fixed $g_\chi = 1$, the plot on the left also sets $g_t = 1$, whilst on the right the top-mediator coupling is weakened to $g_t = 0.1$. In both instances the width is evaluated as the minimal width. The dark matter mass is fixed at $m_{DM} = 100$ GeV, the mediator mass is varied.

In Fig. 10 we show the spin-dependent cross-section limits deduced from the LHC projections and FERMI-LAT now for a light 125 GeV mediator.

V. EFFECTS OF HEAVY NEW PHYSICS ON MEDIATOR PRODUCTION

In this section we investigate potential BSM effects which may alter the production of the dark sector mediator. In particular we focus on additional heavy degrees of freedom, which are charged under $SU(N_c)$. Since we assume that these new degrees of freedom are heavy we can work in the limit in which the new states are integrated out (however, we stress that the mediator remains a propagating particle). This is achieved by including the following interaction in our simplified model Lagrangian in Eq. (1),

$$\mathcal{L}_{\rm EFT} = g_g \frac{\alpha_s}{12\pi v} S \, {\rm Tr}\,(G^{\mu\nu} G_{\mu\nu}) \tag{21}$$

For simplicity we have focused on the scalar mediator, and parameterized the Lagrangian in terms of a rescaled Higgs EFT dimension-5 operator (in which the rescaling factor is g_g). Our extended simplified model now has an additional parameter g_g, resulting in a total of 6 free parameters.

In order to make predictions for the resulting model we need to extend the existing implementation of this process in MCFM [7], which is based upon modified matrix elements for Higgs production (computed originally in ref. [76]). The inclusion of Eq. (21) in the Lagrangian results in a new term which interferes with the top loop contribution at the amplitude level. Accordingly we have recomputed the production amplitude $gg \to g + S$ and $q\overline{q} \to g + S$ in terms of helicity amplitudes. The results for these amplitudes, which to the best of our knowledge, have not been reported elsewhere, are included in the Appendix. Representative Feynman diagrams from this extended model are the first two diagrams in Fig. 1, with the first representing the new BSM contribution assumed to be induced by heavy colored particles.

In Fig. 11 we present the cross section ratio $\sigma(g_g \neq 0)/\sigma(g_g = 0)$ computed in the extended simplified model. Cross sections are obtained using the basic cuts described in section IV, i.e. we require $p_{T,j_1} \geq 110$ GeV and $|\eta| < 2.4$. Since these are LO cross sections, an equivalent cut of 110 GeV is imposed upon the MET. Cross sections are presented for the 14 TeV LHC, and CTEQ6L1 [77] PDF sets have been used, the renormalization and factorization scale are set to $\mu = m_{\chi\overline{\chi}}$. Parametrically we expect a prediction which is of the following form, $a_0 + a_1 g_g + a_2 g_g^2$, and the curves presented in Fig. 11 illustrate this functionality. We have chosen to illustrate two benchmark points, which correspond to a situation in which the (Yukawa adjusted) mediator-top and mediator-DM coupling are set equal ($g_t = g_\chi = 1$),

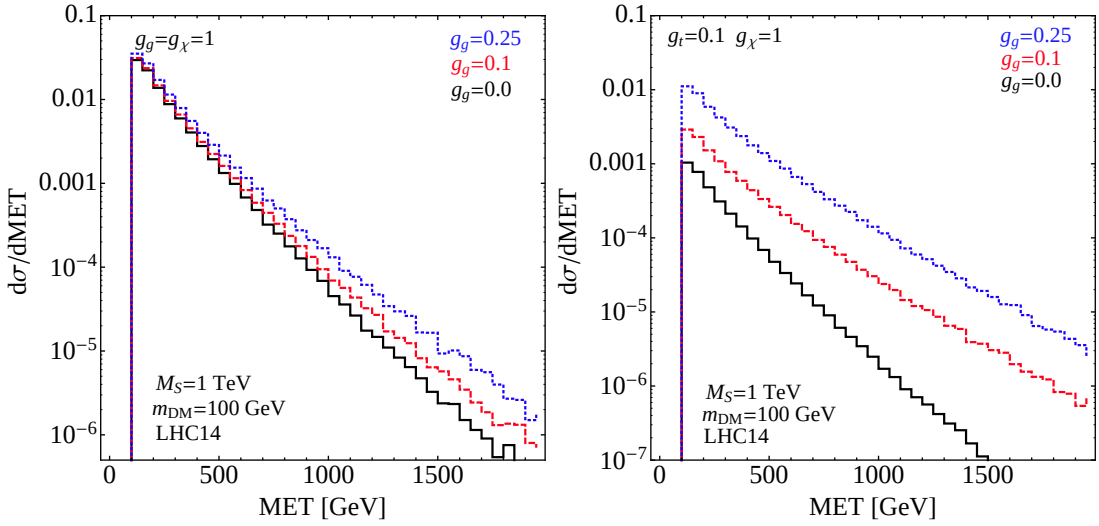

FIG. 12: The missing transverse energy (MET) differential distribution showing parton-level predictions obtained using several choices of g_g for a benchmark scenario in which the dark matter particles 100 GeV and the mediator is 1 TeV. The plot on the left corresponds to the democratic choice of mediator-top and mediator-DM coupling ($g_t = g_\chi = 1$, whilst that on the right corresponds to the case in which $g_t = g_\chi/10 = 0.1$.

and a second scenario in which the coupling to the top is damped $g_t = g_\chi/10 = 0.1$. Clearly in the second scenario we expect a significantly bigger contribution from the heavy particles in the loop, since the top is suppressed. This is illustrated in Fig. 11, for which we see enhancements of order 1-3 for the democratic model, and 10-100 for the top suppressed model. The second case is analogous to the situation in the production of a SM Higgs, in which the propagating b quark loops are suppressed relative to the top quark contribution, which can be evaluated in the heavy top limit. We note that the shapes of the curves in Fig. 11 are dominantly due to the relative importance of g_t compared to g_g, and the mediator mass. The dependence on g_χ cancels in the ratio, as does the decay matrix element to DM, therefore, although we chose a benchmark mass of 10 GeV, Fig. 11 would not be changed if a different m_{DM} were used.

Under the assumption that the scalar mediator proceeds through a portal interaction with the Higgs boson, g_g plays the role of a mixing angle, if g_g becomes large, significant deviations from the SM Higgs should be expected, and have not been observed. If instead the scalar is allowed to couple to the heavy degrees of freedom in an arbitrary way then we interpret g_g as a rescaling factor which relates the coupling and mass scale of the dark sector, to that of the EW scale, i.e.

$$g_g \sim \frac{g_{NP}}{\Lambda_{NP}} \frac{v}{g_w} \tag{22}$$

In order for the EFT to be valid we need to ensure that the kinematic distributions are probed at scales less than Λ_{NP}, we present the differential distribution for the missing transverse momentum in Fig. 12. At 14 TeV the tail of the distribution probes scales of around a few TeV, setting $\Lambda_{NP} = 2$ TeV and assuming g_{NP} is $\mathcal{O}(1)$ we see that the maximum g_g which can be safely probed at the 14 TeV LHC is around $g_g < 0.3$. Figure 12 illustrates the usual result that higher dimensional operators are relatively less suppressed at high energies compared to their four dimensional counterparts, as a result the impact of the g_g pieces can be reinterpreted as momentum dependent form factor which modifies the four-dimensional Lagrangian.

The results presented in this section suggest that, should a propagating resonance be found in the mono-jet channel at the LHC, coupling constraints on loop-induced heavy sector particles can be investigated, of which values approximately $g_g < 0.3$ correspond to theories in which the EFT prescription is viable. These constraints may shed light on extended sectors in the BSM theory which contain heavy colored particles. In addition, if Run II searches based on the simplified models defined in Sec. II lead to null results, then one can also test models in which the scalar mediator, and putative dark matter particles are light, but only couple to the SM through a heavy colored messenger. These instances correspond exactly to the situation in which g_g is non-zero, but $g_t \ll g_g, g_\chi$. In theories with this coupling structure the EFT becomes the dominant production model, and although at the cost of an additional parameter, g_g should be included in the simplified model.

VI. CONCLUSIONS

We have defined benchmark or simplified models for dark particle searches for the cases of scalar, pseudo-scalar, vector and axial-vector mediators between the SM and dark sectors. These models are defined by the interaction in Eqs. (1)-(4) and (21). Apart from the choice of mediator type these models are characterised in our approach by the following free parameters:

1. mediator mass $m_{\rm MED}$
2. mediator width $\Gamma_{\rm MED}$
3. dark matter mass $m_{\rm DM}$
4. effective coupling parameter $g_q \cdot g_\chi$ for scalar and pseudo-scalar mediators (5); and $g_{\rm SM} \cdot g_{\rm DM}$ for axial-vector and vector mediators.

In our examples here we chose to study democratic scenarios in which the couplings in the dark sector and SM were equal, although this need not be the case this reduces the degrees of freedom from 5 to 4. We have implemented simplified models based on these parameters into a fully flexible (and public) Monte Carlo code, MCFM. We used MCFM to generate signal events, which were processed through event and detector simulation for the 8 and 14 TeV LHC. We were then able to use a recent CMS analysis to study benchmark points in our simplified models producing cross section limits, limits in the mediator-dark matter mass plane, and cross section versus mass limits.

The introduction of the simplified models greatly increases the number of free parameters which enter searches at the LHC. Previous iterations of experimental results focused on the regime in which the mediator is assumed to be heavy, such that an effective field theory description is valid. In this setup one has to constrain one parameter per operator, the Wilson coefficient C_i. However at the LHC energies many interesting scenarios occur in which the mediator can be produced on-shell, which makes the introduction of simplified models a useful tool. Future iterations of LHC searches have the harder task of presenting results in this five dimensional plane.

If the simplified model is extended to include coloured degrees of freedom, modifications can occur in the production of the mediating particle. This is particularly relevant for the scalar and pseudo scalar cases, which proceed at the one-loop level. Heavy coloured physics can couple directly to the mediator, and result in an additional 5 dimensional contribution to the Lagrangian. We investigated the impact of this term for the scalar mediated case and found that if the mediator-top coupling is damped then significant contributions to the production cross section can arise from these terms. This is analogous to the situation in the SM, in which the light bottom quark loops are much smaller than the top quark loops (which can be treated in an effective field theory approach).

We find that limitations of direct and indirect detection experiments, i.e. velocity suppression and loop-suppressed couplings to Standard Model particles, can be overcome by LHC searches. Thus, the LHC provides a complementary coverage of the dark sector parameter space with respect to low-energy experiments. Importantly, if the invisible particle is not stable on cosmological time scales the LHC can be the only experiment to probe the dark sector.

The search for dark matter whether in direct, indirect, or collider experiments represents one of the most fascinating, and challenging goals for physics this century. The LHC is about to enter a new era with the start of Run II, and with this the evolution of the LHC searches to incorporate more complete UV models and include the region in which EFT assumptions breakdown, is a natural progression. The simplified models we have discussed here provide a pathway to achieving this.

Note added: When this paper was being finalised, Ref. [14] was posted on the ArXiv, which also considers scalar and pseudo-scalar mediators in the gluon fusion channel and treats $\Gamma_{\rm MED}$ as a free parameter.

Acknowledgments

We would like to thank Brian Batell, Oliver Buchmueller, Albert De Roeck, Patrick Fox, Christopher McCabe, Tim Tait and Christopher Wallace for valuable discussions. The research of VVK and MS is supported by STFC through the IPPP grant and for VVK by the Wolfson Foundation and Royal Society.

Appendix A: Amplitudes for $gg \to S + g$ and $q\bar{q} \to S + g$

In this section we present the helicity amplitudes for $gg \to S + g$ and $q\bar{q} \to S + g$ in both the full and effective field theories. Helicity amplitudes are defined in terms of $u_\pm(k_i)$ where u represents a Weyl spinor of momentum k_i, with

either positive or negative helicity. Basic spinor products are then defined as,

$$\langle ij\rangle = \langle i^-|j^+\rangle = \overline{u}_-(k_i)u_+(k_j), \tag{A1}$$
$$[ij] = \langle i^+|j^-\rangle = \overline{u}_+(k_i)u_-(k_j), \tag{A2}$$

Kinematic invariants are constructed from products of the above quantities,

$$\langle ij\rangle\,[ji] = 2k_ik_j = s_{ij} \tag{A3}$$

Spinor strings are defined as follows,

$$\langle i|P_{kl}|j] = \langle i|(k+l)|j] = \langle ik\rangle\,[kl] + \langle il\rangle\,[lj] \tag{A4}$$

We begin by presenting the $gg \to S + g$ amplitude with a propagating fermion of mass m_f in the loop. We decompose the amplitude in terms of a kinematic primitive amplitude, and normalization factors as follows,

$$A_4(S,1_g^{h_1},2_g^{h_2},3_g^{h_3}) = N_c(N_c^2-1)\frac{g_f m_f^2 g_w}{16\pi^2 M_W}\left(\frac{g_s}{\sqrt{2}}\right)^3 \mathcal{A}(S,1_g^{h_1},2_g^{h_2},3_g^{h_3}) \tag{A5}$$

Of the possible helicity orderings two can be chosen $(+++,\,-++)$ from which all remaining amplitudes can be obtained from conjugation and bose symmetries. The $+++$ amplitude is given in terms of the following box (D_i) and triangle (C_i) scalar integrals

$$\begin{aligned}\mathcal{A}(S,1_g^+,2_g^+,3_g^+) \;=\; &\left(\frac{[21]\,[31]\,(4m_f^2-s_{123})}{\langle 23\rangle}D_1(s_{13},s_{12},m_f^2) + \frac{s_{12}+s_{13}}{\langle 12\rangle\,\langle 13\rangle\,\langle 23\rangle}(4m_f^2-s_{123})C_1(s_{23},s_{123},m_f^2)\right.\\ &\left.+\{1\leftrightarrow 3\}+\{1\leftrightarrow 2\}\right) + \frac{s_{123}}{\langle 12\rangle\,\langle 13\rangle\,\langle 23\rangle}\end{aligned} \tag{A6}$$

Here $D_1(s,t,m_f^2)$ represents a box integral with a single off-shell leg (s_{123}), which is specified completely by s and t channel invariants, $C_1(s,t,m_f^2)$ represents the triangle integral with two legs s and t off-shell. The second helicity amplitude required also contains bubble integrals B_i,

$$\begin{aligned}\mathcal{A}(S,1_g^+,2_g^+,3_g^+) \;=\; &-\frac{\langle 12\rangle\,\langle 13\rangle}{\langle 23\rangle^3}(4s_{12}s_{13}+12m_f^2-s_{23}^2)D_1(s_{13},s_{12},m_f^2) + 2\frac{(s_{12}+s_{13})\,[32]\,(4m_f^2-s_{23})}{\langle 23\rangle^2\,[21]\,[31]}C_1(s_{23},s_{123},m_f^2)\\ &+\left\{\frac{\langle 12\rangle\,[23]^2\,(4m_f^2-s_{23})}{\langle 23\rangle\,[31]}D_1(s_{12},s_{23},m_f^2) + \frac{4\,\langle 12\rangle\,\langle 13\rangle\,s_{13}}{\langle 23\rangle}C_2(s_{13},m_f^2)\right.\\ &+\left(-4\frac{\langle 12\rangle\,\langle 13\rangle\,\langle 3|P_{12}|3]}{\langle 23\rangle^3} + 2\frac{s_{13}\,\langle 13\rangle\,[32]^2}{\langle 23\rangle\,[21]\,\langle 3|P_{12}|3]} - 2\frac{s_{23}\,[23]^3}{[21]\,[31]\,\langle 3|P_{12}|3]}\right.\\ &-4m_f^2\left(2\frac{s_{13}\,\langle 13\rangle\,[32]}{\langle 23\rangle^2\,[21]\,\langle 3|P_{12}|3]} + 4\frac{\langle 13\rangle\,[32]^3}{\langle 23\rangle\,[21]\,\langle 3|P_{12}|3]} + 2\frac{[32]^3}{\langle 3|P_{12}|3]\,[21]\,[31]}\right)\Big)C_1(s_{12},s_{123},m_f^2)\\ &+8\frac{\langle 12\rangle\,\langle 13\rangle\,[32]\,(s_{13}+2s_{123})}{\langle 23\rangle^2\,\langle 3|P_{12}|3]^2}\Big(B_1(s_{12},m_f^2)-B_1(s_{123},m_f^2)\Big)+\{2\leftrightarrow 3\}\Big\}\\ &-\frac{[32]^2\,(s_{12}s_{13}+s_{23}^2)}{\langle 23\rangle\,[21]\,[31]\,\langle 3|P_{12}|3]\langle 2|P_{13}|2]}\end{aligned} \tag{A7}$$

Here we have introduced additional triangle integrals $C_2(s,m_f^2)$ which represent topologies with one off-shell leg (s), and bubble integrals $B_1(s,m_f^2)$ which depend on a scale s. The basis integrals in the above equations can be easily evaluated using public packages, our implementation in MCFM uses QCDLoop [78].

The amplitude for $q\overline{q} \to S + g$ can be written as follows,

$$A_4(S,1_{\overline{q}}^{h_1},2_q^{-h_1},3_g^{h_3}) = (N_c^2-1)\frac{g_f m_f^2 g_w g_s^3}{16\pi^2 M_W}\mathcal{A}(S,1_{\overline{q}}^{h_1},2_q^{-h_1},3_g^{h_3}) \tag{A8}$$

here the primitive amplitude can be defined in terms of one helicity configuration $(-++)$ with all other configurations obtainable from line reversal and conjugation symmetries. Our primitive amplitude is

$$\begin{aligned}\mathcal{A}(1_{\overline{q}}^-,2_q^+,3+) \;=\; &2\frac{[23]^2}{[21]}(\langle 3|P_{12}|3] - 4m_f^2)C_1(s_{12},s_{123},m_f^2)\\ &-4\frac{\langle 12\rangle\,[32]^2}{\langle 3|P_{12}|3]^2}(B_1(s_{12},m_f^2)-B_1(s_{123},m_f^2)+4\frac{[32]^2}{[21]\,\langle 3|P_{12}|3]}\end{aligned} \tag{A9}$$

In addition to the amplitudes presented above, we will also need the $m_f \to \infty$ limit, which corresponds to amplitudes computed in the effective field theory. These amplitudes have been computed in ref. [79], and have the following form,

$$\mathcal{A}_{m_f\to\infty}(S, 1_g^+, 2_g^+, 3_g^+) = \frac{s_{123}^2}{\langle 12\rangle \langle 23\rangle \langle 31\rangle} \tag{A10}$$

$$\mathcal{A}_{m_f\to\infty}(S, 1_g^+, 2_g^-, 3_g^-) = \frac{\langle 23\rangle^2}{\langle 12\rangle \langle 31\rangle} \tag{A11}$$

[1] D. Alves *et al.* [LHC New Physics Working Group Collaboration], J. Phys. G **39**, 105005 (2012) [arXiv:1105.2838 [hep-ph]].
[2] J. Abdallah, A. Ashkenazi, A. Boveia, G. Busoni, A. De Simone, C. Doglioni, A. Efrati and E. Etzion *et al.*, arXiv:1409.2893 [hep-ph].
[3] S. Malik, C. McCabe, H. Araujo, A. Belyaev, C. Boehm, J. Brooke, O. Buchmueller, G. Davies, *et al.*, arXiv:1409.4075 [hep-ex].
[4] P. J. Fox, R. Harnik, J. Kopp and Y. Tsai, Phys. Rev. D **84**, 014028 (2011) [arXiv:1103.0240 [hep-ph]].
[5] P. J. Fox, R. Harnik, J. Kopp and Y. Tsai, Phys. Rev. D **85** (2012) 056011 arXiv:1109.4398 [hep-ph].
[6] U. Haisch, F. Kahlhoefer and J. Unwin, JHEP **1307**, 125 (2013) [arXiv:1208.4605 [hep-ph]].
[7] P. J. Fox and C. Williams, Phys. Rev. D **87**, no. 5, 054030 (2013) [arXiv:1211.6390 [hep-ph]].
[8] H. An, X. Ji and L. T. Wang, JHEP **1207** (2012) 182 [arXiv:1202.2894 [hep-ph]].
[9] O. Buchmueller, M. J. Dolan and C. McCabe, JHEP **1401** (2014) 025 arXiv:1308.6799 [hep-ph].
[10] A. Alves, S. Profumo and F. S. Queiroz, JHEP **1404**, 063 (2014) [arXiv:1312.5281 [hep-ph]].
[11] G. Arcadi, Y. Mambrini, M. H. G. Tytgat and B. Zaldivar, JHEP **1403**, 134 (2014) [arXiv:1401.0221 [hep-ph]].
[12] F. Richard, G. Arcadi and Y. Mambrini, arXiv:1411.0088 [hep-ex].
[13] O. Buchmueller, M. J. Dolan, S. A. Malik and C. McCabe, arXiv:1407.8257 [hep-ph].
[14] M. R. Buckley, D. Feld and D. Goncalves, arXiv:1410.6497 [hep-ph].
[15] C. Englert, J. Jaeckel, E. Re and M. Spannowsky, Phys. Rev. D **85**, 035008 (2012) [arXiv:1111.1719 [hep-ph]].
[16] G. Aad *et al.* [ATLAS Collaboration], Phys. Lett. B **705**, 294 (2011) [arXiv:1106.5327 [hep-ex]].
[17] J. M. Campbell and R. K. Ellis, Phys. Rev. D **60**, 113006 (1999) [hep-ph/9905386].
[18] J. M. Campbell, R. K. Ellis and C. Williams, JHEP **1107**, 018 (2011) [arXiv:1105.0020 [hep-ph]].
[19] J. M. Campbell, R. K. Ellis and C. Williams, MCFM website http://mcfm.fnal.gov
[20] U. Haisch, F. Kahlhoefer and E. Re, JHEP **1312**, 007 (2013) [arXiv:1310.4491 [hep-ph], arXiv:1310.4491].
[21] T. Aaltonen *et al.* [CDF Collaboration], Phys. Rev. Lett. **108**, 211804 (2012) [arXiv:1203.0742 [hep-ex]].
[22] S. Chatrchyan *et al.* [CMS Collaboration], JHEP **1209**, 094 (2012) [arXiv:1206.5663 [hep-ex]].
[23] [ATLAS Collaboration], Conference paper ATLAS-CONF-2012-084.
[24] V. Khachatryan *et al.* [CMS Collaboration], arXiv:1408.3583 [hep-ex].
[25] E. Diehl [ATLAS Collaboration], AIP Conf. Proc. **1604**, 324 (2014).
[26] V. D. Barger, K. Hagiwara, J. Woodside and W. Y. Keung, Phys. Rev. Lett. **53**, 641 (1984).
[27] E. W. N. Glover, A. D. Martin and M. R. Pennington, Phys. Lett. B **153**, 330 (1985).
[28] L. J. Hall and A. E. Nelson, Phys. Lett. B **153**, 430 (1985).
[29] J. L. Feng, S. Su and F. Takayama, Phys. Rev. Lett. **96**, 151802 (2006) [hep-ph/0503117].
[30] Q. H. Cao, C. R. Chen, C. S. Li and H. Zhang, JHEP **1108**, 018 (2011) [arXiv:0912.4511 [hep-ph]].
[31] M. Beltran, D. Hooper, E. W. Kolb, Z. A. C. Krusberg and T. M. P. Tait, JHEP **1009**, 037 (2010) [arXiv:1002.4137 [hep-ph]].
[32] V. M. Abazov *et al.* [D0 Collaboration], Phys. Rev. Lett. **90**, 251802 (2003) [hep-ex/0302014].
[33] L. J. Hall and J. Polchinski, Phys. Lett. B **152**, 335 (1985).
[34] J. F. Gunion and S. Mrenna, Phys. Rev. D **64**, 075002 (2001) [hep-ph/0103167].
[35] H. K. Dreiner, M. Kramer and J. Tattersall, Europhys. Lett. **99**, 61001 (2012) [arXiv:1207.1613 [hep-ph]].
[36] J. Goodman, M. Ibe, A. Rajaraman, W. Shepherd, T. M. P. Tait and H. B. Yu, Phys. Lett. B **695**, 185 (2011) [arXiv:1005.1286 [hep-ph]].
[37] J. Goodman, M. Ibe, A. Rajaraman, W. Shepherd, T. M. P. Tait and H. B. Yu, Phys. Rev. D **82**, 116010 (2010) [arXiv:1008.1783 [hep-ph]].
[38] C. Englert and M. Spannowsky, arXiv:1408.5147 [hep-ph].
[39] G. Busoni, A. De Simone, E. Morgante and A. Riotto, Phys. Lett. B **728**, 412 (2014) [arXiv:1307.2253 [hep-ph]].
[40] M. Papucci, A. Vichi and K. M. Zurek, arXiv:1402.2285 [hep-ph].
[41] G. Busoni, A. De Simone, J. Gramling, E. Morgante and A. Riotto, JCAP **1406**, 060 (2014) [arXiv:1402.1275 [hep-ph]].
[42] U. Haisch, A. Hibbs and E. Re, Phys. Rev. D **89**, no. 3, 034009 (2014) [arXiv:1311.7131 [hep-ph]].
[43] G. D'Ambrosio, G. F. Giudice, G. Isidori and A. Strumia, Nucl. Phys. B **645**, 155 (2002) [hep-ph/0207036].
[44] C. Englert, J. Jaeckel, V. V. Khoze and M. Spannowsky, JHEP **1304** (2013) 060 [arXiv:1301.4224 [hep-ph]].
[45] C. Englert, T. Plehn, D. Zerwas and P. M. Zerwas, Phys. Lett. B **703**, 298 (2011) [arXiv:1106.3097 [hep-ph]].
[46] V. V. Khoze, JHEP **1311** (2013) 215 [arXiv:1308.6338 [hep-ph]].

[47] T. Hambye and A. Strumia, Phys. Rev. D **88** (2013) 055022 [arXiv:1306.2329 [hep-ph]].
[48] V. V. Khoze, C. McCabe and G. Ro, JHEP **1408** (2014) 026 [arXiv:1403.4953 [hep-ph], arXiv:1403.4953].
[49] W. Altmannshofer, W. A. Bardeen, M. Bauer, M. Carena and J. D. Lykken, arXiv:1408.3429 [hep-ph].
[50] M. Heikinheimo, A. Racioppi, M. Raidal, C. Spethmann and K. Tuominen, Nucl. Phys. B **876**, 201 (2013) [arXiv:1305.4182 [hep-ph]].
[51] E. Gabrielli, M. Heikinheimo, K. Kannike, A. Racioppi, M. Raidal and C. Spethmann, Phys. Rev. D **89** (2014) 015017 [arXiv:1309.6632 [hep-ph]].
[52] M. Duerr, P. Fileviez Perez and M. B. Wise, Phys. Rev. Lett. **110**, 231801 (2013) [arXiv:1304.0576 [hep-ph]].
[53] M. Duerr and P. Fileviez Perez, Phys. Lett. B **732**, 101 (2014) [arXiv:1309.3970 [hep-ph]].
[54] S. R. Coleman and E. J. Weinberg, Phys. Rev. D **7** (1973) 1888.
[55] D. S. Akerib *et al.* [LUX Collaboration], Nucl. Instrum. Meth. A **704**, 111 (2013) [arXiv:1211.3788 [physics.ins-det]].
[56] D. S. Akerib *et al.* [LUX Collaboration], Phys. Rev. Lett. **112**, no. 9, 091303 (2014) [arXiv:1310.8214 [astro-ph.CO]].
[57] M. Szydagis *et al.* [LUX Collaboration], arXiv:1402.3731 [hep-ex].
[58] A. Kurylov and M. Kamionkowski, Phys. Rev. D **69**, 063503 (2004) [hep-ph/0307185].
[59] J. Hisano, K. Ishiwata and N. Nagata, Phys. Rev. D **82**, 115007 (2010) [arXiv:1007.2601 [hep-ph]].
[60] K. Cheung, C. T. Lu, P. Y. Tseng and T. C. Yuan, arXiv:1308.0067 [hep-ph].
[61] H. Y. Cheng and C. W. Chiang, JHEP **1207**, 009 (2012) [arXiv:1202.1292 [hep-ph]].
[62] K. R. Dienes, J. Kumar, B. Thomas and D. Yaylali, Phys. Rev. D **90**, 015012 (2014) [arXiv:1312.7772 [hep-ph]].
[63] S. Archambault *et al.* [PICASSO Collaboration], Phys. Lett. B **711**, 153 (2012) [arXiv:1202.1240 [hep-ex]].
[64] E. Behnke *et al.* [COUPP Collaboration], Phys. Rev. D **86**, 052001 (2012) [arXiv:1204.3094 [astro-ph.CO]].
[65] M. Felizardo, T. A. Girard, T. Morlat, A. C. Fernandes, A. R. Ramos, J. G. Marques, A. Kling and J. Puibasset *et al.*, Phys. Rev. Lett. **108**, 201302 (2012) [arXiv:1106.3014 [astro-ph.CO]].
[66] M. Ackermann *et al.* [Fermi-LAT Collaboration], Phys. Rev. Lett. **107**, 241302 (2011) [arXiv:1108.3546 [astro-ph.HE]].
[67] A. A. Abdo *et al.* [Fermi-LAT Collaboration], Astrophys. J. **712**, 147 (2010) [arXiv:1001.4531 [astro-ph.CO]].
[68] J. M. Zheng, Z. H. Yu, J. W. Shao, X. J. Bi, Z. Li and H. H. Zhang, Nucl. Phys. B **854**, 350 (2012) [arXiv:1012.2022 [hep-ph]].
[69] C. Boehm, M. J. Dolan, C. McCabe, M. Spannowsky and C. J. Wallace, JCAP **1405**, 009 (2014) [arXiv:1401.6458 [hep-ph]].
[70] T. Sjstrand, S. Ask, J. R. Christiansen, R. Corke, N. Desai, P. Ilten, S. Mrenna and S. Prestel *et al.*, arXiv:1410.3012 [hep-ph].
[71] M. Cacciari, G. P. Salam and G. Soyez, Eur. Phys. J. C **72**, 1896 (2012) [arXiv:1111.6097 [hep-ph]].
[72] V. Khachatryan *et al.* [CMS Collaboration], CMS-JME-10-011 arXiv:1107.4277 [physics.ins-det].
[73] V. Khachatryan *et al.* [CMS Collaboration], CERN-PH-EP-2014-246, CMS-PAS-JME-13-003-003
[74] J. Alwall, M. Herquet, F. Maltoni, O. Mattelaer and T. Stelzer, JHEP **1106**, 128 (2011) [arXiv:1106.0522 [hep-ph]].
[75] N. Kidonakis, Phys. Rev. D **82**, 114030 (2010) [arXiv:1009.4935 [hep-ph]].
[76] R. K. Ellis, I. Hinchliffe, M. Soldate and J. J. van der Bij, Nucl. Phys. B **297**, 221 (1988).
[77] H. L. Lai, M. Guzzi, J. Huston, Z. Li, P. M. Nadolsky, J. Pumplin and C.-P. Yuan, Phys. Rev. D **82**, 074024 (2010) [arXiv:1007.2241 [hep-ph]].
[78] R. K. Ellis and G. Zanderighi, JHEP **0802**, 002 (2008) [arXiv:0712.1851 [hep-ph]].
[79] S. D. Badger, E. W. N. Glover and V. V. Khoze, JHEP **0503**, 023 (2005) [hep-th/0412275].